FRACTIONAL BIORTHOGONAL PARTNERS IN CHANNEL EQUALIZATION AND SIGNAL INTERPOLATION*

Bojan Vrcelj and P. P. Vaidyanathan
Contact Author: P. P. Vaidyanathan, Department of Electrical Engineering 136-93,
California Institute of Technology, Pasadena, CA 91125 USA,
Phone: (626) 395-4681 E-mail: ppvnath@systems.caltech.edu

December 18, 2002

EDICS number: 2-MWAV

ABSTRACT

The concept of biorthogonal partners has been introduced recently by the authors. The work presented here is an extension of some of these results to the case where the upsampling and downsampling ratios are not integers but rational numbers. Hence the name fractional biorthogonal partners. The conditions for the existence of stable and of FIR fractional biorthogonal partners are derived. It is also shown that the FIR solutions (when they exist) are not unique. This property is further explored in one of the applications of fractional biorthogonal partners, namely the fractionally spaced equalization in digital communications. The goal is to construct zero-forcing equalizers that also combat the channel noise. The performance of these equalizers is assessed through computer simulations. Another application considered is the all-FIR interpolation technique with the minimum amount of oversampling required in the input signal. We also consider the extension of the least squares approximation problem to the setting of fractional biorthogonal partners.

*Work supported in part by the ONR grant N00014-99-1-1002, USA.

1 Introduction

The concept of biorthogonal partners has been introduced recently by the authors in both the scalar [21] and the vector cases [26, 28]. Two digital filters $H(z)$ and $F(z)$ are called biorthogonal partners of each other with respect to an integer M if their cascade $H(z)F(z)$ obeys the Nyquist(M) property. The application of biorthogonal partners in the reconstruction of signals oversampled by integer amounts has been proposed in [21]. In this paper we consider an extension of the same reasoning to the signals oversampled by fractional amounts. This gives rise to the definition of *fractional* biorthogonal partners (**FBP**s in the following), introduced recently in [23, 24].

We start by providing a motivation for the study of FBPs and defining them formally. Next we show a way to construct fractional biorthogonal partners. This discussion leads to deriving the conditions for the existence of FIR FBPs and of stable FBPs. An immediate consequence of the construction procedure is that FIR FBPs (when they exist) are not unique. This property becomes very useful in the first application of FBPs that we consider, namely the channel equalization in digital communication systems using *fractionally spaced equalizers* (**FSE**s). It is shown that, if the amount of oversampling at the receiver is a *rational number*, the problem can be posed in terms of fractional biorthogonal partners. The advantage is that many results developed in this and similar settings can be employed in order to find a fractionally spaced equalizer. Moreover, given the nonuniqueness of such solutions, it is possible to pose the problem of finding a fractionally spaced equalizer that in addition to being zero-forcing also combats the channel noise. This construction method is considered next and the performance of the equalizer is evaluated through computer simulations. Another application of FBPs considered here is the spline interpolation. We show that it is possible to interpolate a slightly oversampled signal using exclusively FIR filtering. This technique is illustrated by an image interpolation example. We also consider the least squares approximation problem in the setting of fractional biorthogonal partners.

1.1 Paper outline and relation to past work

The relation between biorthogonal partners and biorthogonal filter banks was pointed out in [21]. An extension of filter banks to the case when the decimation ratios in subbands are rational numbers instead of integers, namely perfect reconstruction *rational* filter banks were treated by many authors [9, 7]. It can be shown that every pair of filters $\{H_k(z), F_k(z)\}$ in a perfect reconstruction rational filter bank forms a *fractional biorthogonal partner* pair. However, the properties of such filters considered *outside* the filter bank setup were not addressed previously and constitute a major part

of this work. In addition to this, the reader will find that the theory as well as the applications presented in this paper are quite different from the results on rational PR filter banks and are more related to the theory of biorthogonal [21] and MIMO biorthogonal partners [26].

In Sec. 2 we introduce the precise definition of fractional biorthogonal partners. We describe the construction procedure for finding a FBP of a discrete-time filter $F(z)$. Moreover, we derive a set of necessary and sufficient conditions for the existence of stable and of FIR FBPs. One of the results which follow from this derivation is that FIR FBPs (if they exist) are not unique.

Sec. 3 considers one of the applications of FBPs - the channel equalization with fractionally spaced equalizers. The idea of signal oversampling at the receiver for the purpose of FIR equalization is well-known to the signal processing community (see the tutorial paper by Treichler *et al.* [17] and references therein). The same idea has also been used for blind channel identification [16, 13, 14]. In the context of FBPs we are interested in fractionally spaced equalizers with *fractional* amount of oversampling at the receiver. After reviewing the characteristics of FSEs, especially those with fractional amount of oversampling, we draw a parallel between FSEs and FBPs. We show that it is possible to optimize FIR FBPs such that when acting as zero-forcing FSEs they also reduce the noise power at the receiver. The performance of such optimized equalizers is evaluated in the section with experimental results where we compare it to the performance of several other equalization methods including the minimum mean-squared error (MMSE) equalizer.

In Sec. 4 we consider another application of FBPs, namely the interpolation of signals described by oversampled models. This method is a modification of the well-known spline interpolation technique [4, 12] which requires the use of non-causal IIR filters. Efficient implementation of this filtering is treated in [18]. Here we show that by assuming even a slightly oversampled model for the signal, *exact* spline interpolation is possible using only FIR filters. This approach is thus different from another all-FIR spline interpolation method described in [22] where certain approximations were introduced.

Approximation of arbitrary signals by signals admitting a described oversampled model is treated in Sec. 5. This discussion is an extension to rational oversampling ratios of similar methods treated in [18, 21] and is also closely related to the concept of oblique projections [2]. The solution to this problem involves the use of fractional biorthogonal partners. This solution will make use of the corresponding results in the MIMO biorthogonal partner case [26], even though the initial problem formulations seem quite different. In Sec. 6 we extend some of the scalar results derived previously to the case of vector signals.

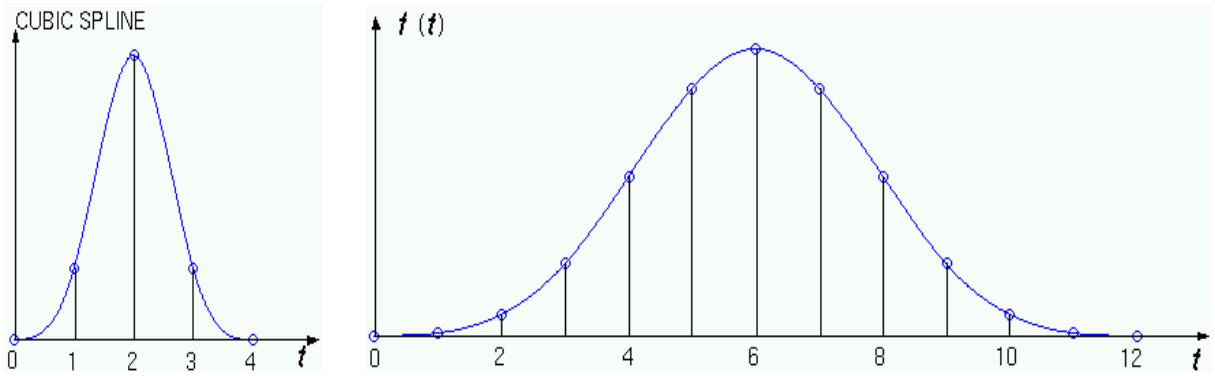

Figure 1: Example of a generating function $\phi(t)$ (cubic spline) and its three times "stretched" version $f(t)$.

1.2 Notations

If not stated otherwise, all notations are as in [19]. We use the notation $[x(n)]_{\downarrow M}$ and $[X(z)]_{\downarrow M}$ to denote the decimated version $x(Mn)$ and its z-transform. The expanded version

$$\begin{cases} x(n/M) & \text{for } n = \text{mul of } M, \\ 0 & \text{otherwise} \end{cases}$$

is similarly denoted by $[x(n)]_{\uparrow M}$, and its z-transform $X(z^M)$ denoted by $[X(z)]_{\uparrow M}$. In a block diagram, the scalar decimation and expansion operations will be denoted by encircled symbols $\downarrow M$ and $\uparrow M$ respectively. In the case of vectors and matrices, the decimation and expansion are performed on each element separately. The corresponding vector sequence decimation/expansion symbols are placed in square boxes.

The polyphase decomposition [19] will play a significant role in the following. If $F(z)$ is a transfer function, then it can be written in the Type-1 polyphase form as

$$F(z) = \sum_{k=0}^{M-1} z^{-k} F_k(z^M), \tag{1}$$

and a similar expression denotes the Type-2 polyphase form.

2 Fractional Biorthogonal Partners

Biorthogonal partners as originally introduced in [21] arise in many different contexts. One of them is the reconstruction of continuous time signals admitting the model

$$x(t) = \sum_{k=-\infty}^{\infty} c(k)\phi(t-k). \tag{2}$$

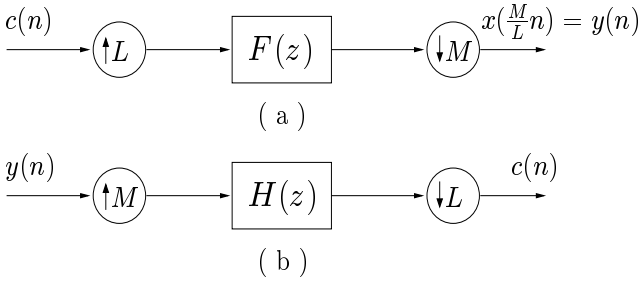

Figure 2: (a) Signal model. (b) Scheme for reconstruction.

Given the integer samples of $x(t)$ admitting the model (2), namely

$$x(n) = \sum_{k=-\infty}^{\infty} c(k)\phi(n-k) \tag{3}$$

the reconstruction of the driving sequence $c(n)$ and thus of $x(t)$ is obtained by inverse filtering $1/\Phi(z)$, with $\Phi(z)$ denoting the z-transform of $\phi(n)$. This is a direct consequence of (3). It has been shown [21] that the IIR reconstructive filtering $1/\Phi(z)$ can often be replaced by simple FIR filtering if the continuous time signal $x(t)$ is sampled L times more densely (for an integer $L \geq 2$). The FIR filter used for reconstruction in that case is called a biorthogonal partner [21] of the corresponding oversampled version of $\Phi(z)$ with respect to an integer L. In the following we consider the case where $x(t)$ is oversampled by a rational number, possibly less than two. We shall see that FIR reconstruction is often possible even under these relaxed conditions.

Suppose we are given the discrete time signal $y(n)$ that is obtained by sampling $x(t)$ from (2) at the rate L/M, i.e. $y(n) = x(nM/L)$. For obvious reasons we will assume that M and L are coprime. We shall see later that in most of the applications considered here $L > M$ is required as well, although in principle it is not necessary. Notice that $y(n)$ is obtained by *oversampling* $x(t)$ with respect to the usual integral sampling strategy by a factor of L/M. Therefore we have

$$\begin{aligned} y(n) &= x(\frac{M}{L}n) = \sum_{k=-\infty}^{\infty} c(k)\phi(\frac{M}{L}n - k) \\ &= \sum_{k=-\infty}^{\infty} c(k) f(Mn - kL), \end{aligned} \tag{4}$$

where $f(t) \stackrel{\triangle}{=} \phi(t/L)$ is the generating function "stretched" by a factor of L. This is shown in Fig. 1 for the case where $\phi(t)$ is a cubic spline [4] and $L = 3$. The signal $y(n)$ from (4) can thus be obtained as shown in Fig. 2(a).

Now consider the problem of signal reconstruction [recovering $c(n)$ from $y(n)$]. We look for the solution of the form depicted in Fig. 2(b). It will be shown that under some mild assumptions

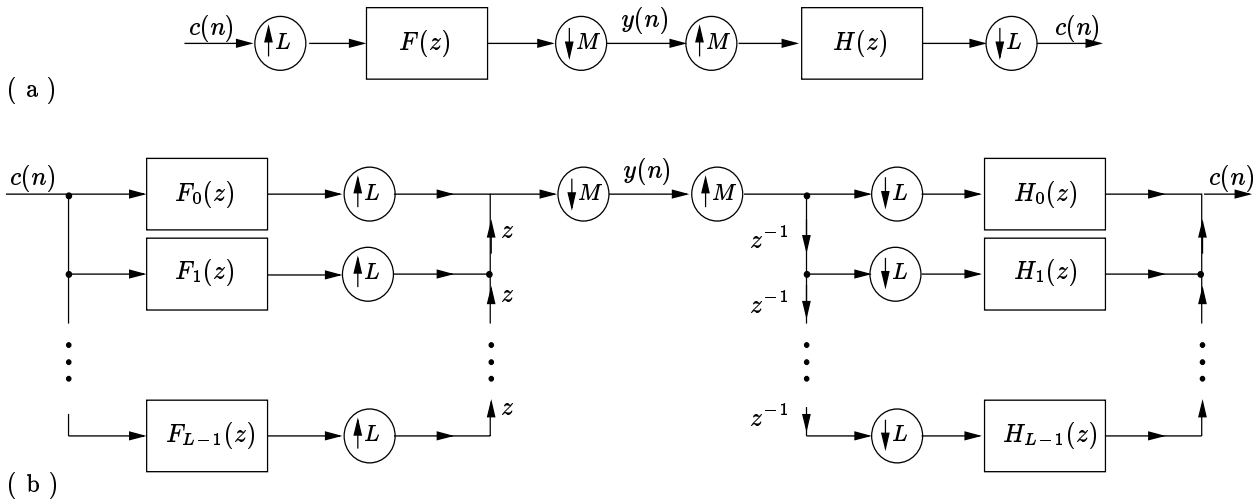

Figure 3: (a)-(b) Equivalent presentations of fractional biorthogonal partners.

this solution [i.e. filter $H(z)$] exists. Further, we establish the conditions under which an FIR filter $F(z)$ yields an FIR solution for $H(z)$.

2.1 Definition

The preceding discussion leads naturally to the definition of fractional biorthogonal partners.

Definition. Transfer function $H(z)$ is said to be a *right fractional biorthogonal partner* (RFBP) of $F(z)$ with respect to the fraction L/M if the system shown in Fig. 3(a) is identity. Under these conditions $F(z)$ is also said to be a *left fractional biorthogonal partner* (LFBP) of $H(z)$ with respect to L/M.

This definition includes the notion of (integral) biorthogonal partners [21] as a special case when $M = 1$. Note that the system in Fig. 3(a) becomes linear time invariant (LTI) whenever M divides L, while in general it is not. Also, note that (as opposed to the $M = 1$ case) we need to distinguish between left and right FBPs. However, the results that hold for RFBPs can easily be modified to accommodate LFBPs, and therefore we only focus on RFBPs in the following. It is important to note the distinction between this definition and a similar definition of left (right) biorthogonal partners in the MIMO case [26]. Right FBP appears on the right-hand side in the *diagram* in Fig. 3(a), while right MIMO biorthogonal partner appears on the right-hand side in the equivalent *transfer function* (thus on the left-hand side in the diagram). The reason for this inconsistency is that in general for $M > 1$ the system with fractional biorthogonal partners in Fig. 3(a) is not LTI, so we cannot write its transfer function. As a final remark, note that if the fraction

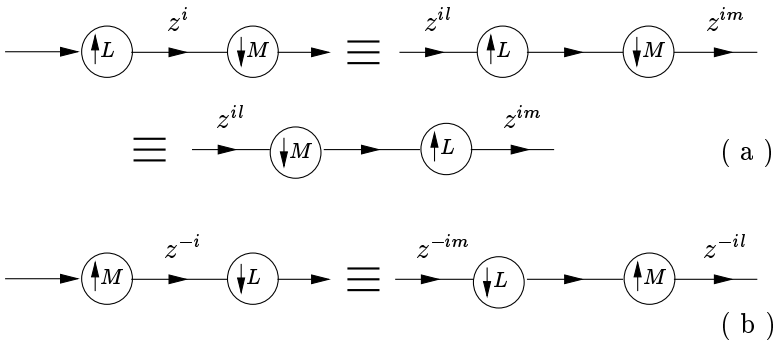

Figure 4: (a)-(b) Some multirate identities.

L/M is changed, the two filters may not remain FBPs, but we will avoid mentioning this fraction whenever no confusion is anticipated.

Returning to the previous discussion we see that the reconstruction of $x(t)$ given by the model (2) from its samples $y(n)$ obtained at rate L/M is possible if $F(z)$ has a stable RFBP $H(z)$. Similarly, it is possible to perform an FIR reconstruction whenever there exists an FIR RFBP. In the following we describe a way of constructing fractional biorthogonal partners. This will result in a set of conditions for the existence of FIR or just stable FBPs.

2.2 Existence and construction of FBPs

Consider the system in Fig. 3(a). Write the filters $F(z)$ and $H(z)$ in terms of their Type-2 and Type-1 polyphase components [19]

$$F(z) = \sum_{k=0}^{L-1} F_k(z^L) z^k, \quad \text{and} \quad H(z) = \sum_{k=0}^{L-1} H_k(z^L) z^{-k}. \tag{5}$$

Then we can redraw the system as shown in Fig. 3(b). Next, consider the left-hand side of Fig. 3(b) and focus on the system between the output of the ith filter $F_i(z)$ and $y(n)$. This is given by a cascade of an expander by L, advance operator z^i and a decimator by M [see Fig. 4(a)]. Since we assumed M and L are coprime, there exist integers m and l such that

$$lL + mM = 1. \tag{6}$$

In fact, the unique solution for the smallest m and l can be obtained by the Euclid's algorithm. Writing the delay $z^i = z^{ilL} \cdot z^{imM}$, we can easily prove the multirate identity depicted in Fig. 4(a). Similarly, we can show that the system between $y(n)$ and the input to $H_i(z)$ can be equivalently redrawn as in Fig. 4(b).

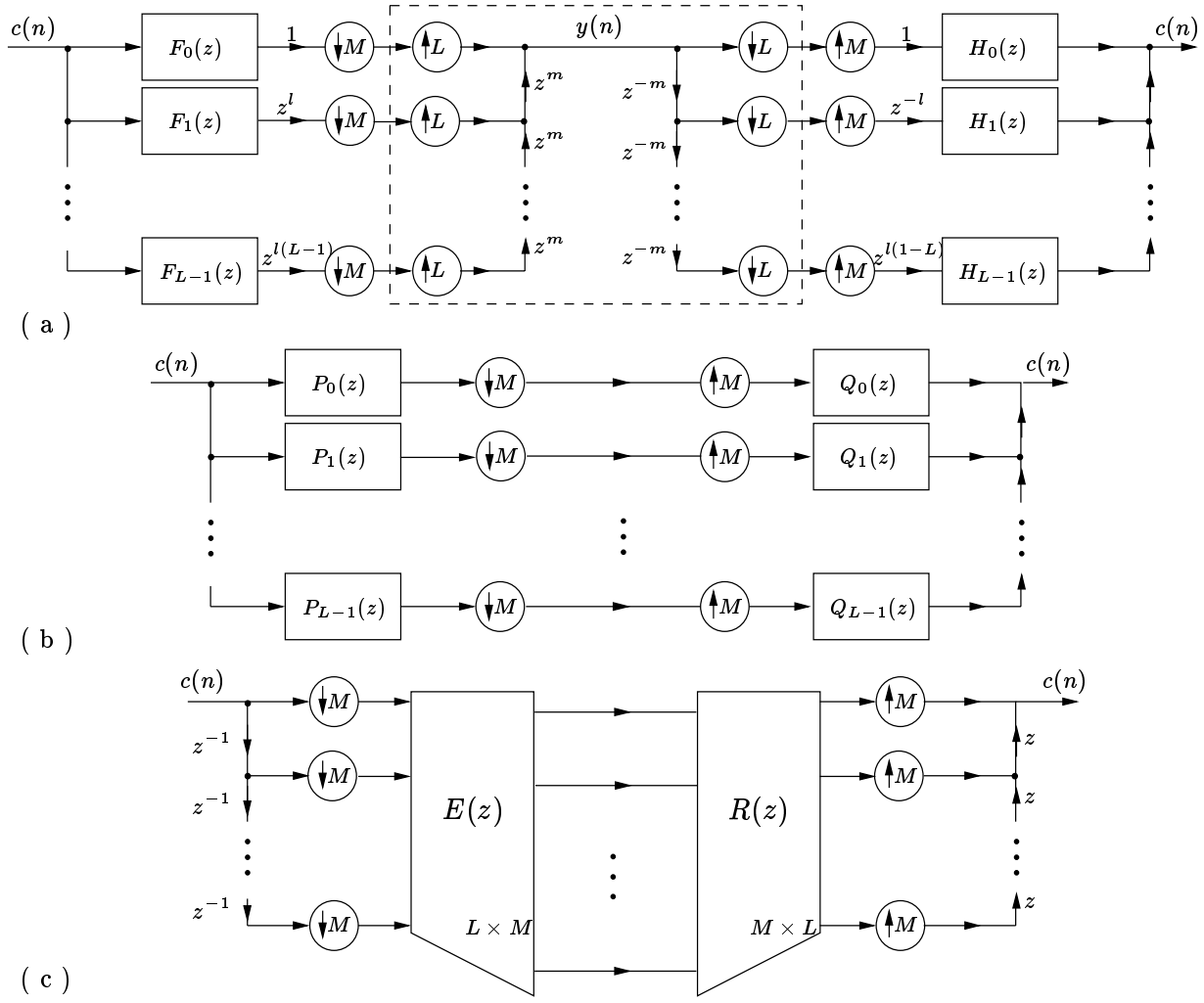

Figure 5: (a)-(c) Further simplifications of fractional biorthogonal partners.

Substituting the described identities back to Fig. 3(b) we obtain the equivalent structure shown in Fig. 5(a). Let us define

$$P_k(z) \stackrel{\triangle}{=} z^{kl} F_k(z), \quad \text{and} \quad Q_k(z) \stackrel{\triangle}{=} z^{-kl} H_k(z), \tag{7}$$

for $0 \leq k \leq L-1$. Since L and M are coprime, it follows that L and m are coprime as well. Under these circumstances it can be shown that the $L \times L$ system shown in Fig. 5(a) within the dashed box is the identity. Thus, the whole structure can be redrawn as in Fig. 5(b). It is important to notice here that the original filters $F(z)$ and $H(z)$ are FIR if and only if the banks of filters $\{P_k(z)\}$ and $\{Q_k(z)\}$ are FIR for all k. The structure from Fig. 5(b) is an L-channel, uniform, nonmaximally decimated filter bank. In our setting one side (analysis or synthesis) of this filter bank is usually known, and the task is to construct the other side so that the whole system has

perfect reconstruction (PR) [19] property. For example, in the problem of signal reconstruction, $F(z)$ and thus $\{P_k(z)\}$ are known and the goal is to find the corresponding synthesis bank $\{Q_k(z)\}$. Recall that at the same time this is exactly the problem of constructing a RFBP $H(z)$, since it is uniquely defined by the filters $\{Q_k(z)\}$. The solution to this problem is well-known to the signal processing community. First, we define the $L \times M$ analysis and the $M \times L$ synthesis polyphase matrices $\mathbf{E}(z)$ and $\mathbf{R}(z)$ respectively

$$\begin{aligned}
\mathbf{E}(z) &= \begin{bmatrix} E_{0,0}(z) & E_{0,1}(z) & \cdots & E_{0,M-1}(z) \\ E_{1,0}(z) & E_{1,1}(z) & \cdots & E_{1,M-1}(z) \\ \vdots & \vdots & \vdots & \vdots \\ E_{L-1,0}(z) & E_{L-1,1}(z) & \cdots & E_{L-1,M-1}(z) \end{bmatrix}, \\
\mathbf{R}(z) &= \begin{bmatrix} R_{0,0}(z) & R_{0,1}(z) & \cdots & R_{0,L-1}(z) \\ R_{1,0}(z) & R_{1,1}(z) & \cdots & R_{1,L-1}(z) \\ \vdots & \vdots & \vdots & \vdots \\ R_{M-1,0}(z) & R_{M-1,1}(z) & \cdots & R_{M-1,L-1}(z) \end{bmatrix}
\end{aligned} \tag{8}$$

containing the Type-1 and Type-2 polyphase components (of order M this time) $E_{i,j}(z)$ and $R_{i,j}(z)$ defined by

$$P_k(z) = \sum_{j=0}^{M-1} E_{k,j}(z^M) z^{-j}, \quad \text{and} \quad Q_k(z) = \sum_{i=0}^{M-1} R_{i,k}(z^M) z^i, \tag{9}$$

for $0 \leq k \leq L-1$. Now the system in Fig. 5(b) can be equivalently redrawn as in Fig. 5(c). We see that the problem of finding a RFBP of $F(z)$ becomes equivalent to that of finding a *left inverse* $\mathbf{R}(z)$ of an $L \times M$ matrix $\mathbf{E}(z)$. Obviously, when computing a LFBP, we would need to find a right matrix inverse of $\mathbf{R}(z)$. At this point it should be clear why the condition $L > M$ was included in the problem formulation. For $L < M$, the polyphase matrices $\mathbf{E}(z)$ and $\mathbf{R}(z)$ do not have the corresponding inverses; in other words, there is not enough information in the samples $y(n)$ to reconstruct $x(t)$. On the other hand, when $L = M$ the system in Fig. 3(a) is just a cascade of two LTI systems [namely the zeroth polyphase components of $F(z)$ and $H(z)$], so the unique FBP is obtained by filter inversion. Based on the previous findings we prove the following theorem.

Theorem 1. Given the transfer function $F(z)$ and two coprime integers L and M, there exists a *stable* right fractional biorthogonal partner of $F(z)$ if and only if $L > M$, and the minimum rank of $\mathbf{E}(e^{j\omega})$ pointwise in ω is M. For an FIR filter $F(z)$ there exists an *FIR* right fractional biorthogonal partner if and only if $L > M$, and the greatest common divisor (gcd) of all the $M \times M$ minors of $\mathbf{E}(z)$ is a delay. Here, the polyphase matrix $\mathbf{E}(z)$ is defined by (8)-(9). Analogous results hold for left FBPs as well.

Proof. We have shown that there exists a stable (FIR) RFBP of $F(z)$ if and only if there exists a stable (polynomial) left inverse of a (polynomial) matrix $\mathbf{E}(z)$. We know that fat matrices do not

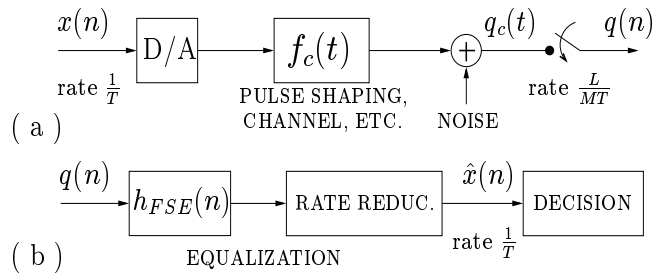

Figure 6: Continuous time communication system. (a) Transmitter and channel. (b) Receiver.

have a left inverse, so we immediately have $L > M$ as a necessary condition ($L = M$ is eliminated for the reasons explained earlier). Next, for the inverse of $\mathbf{E}(e^{j\omega})$ to be stable, we need the full column rank of $\mathbf{E}(e^{j\omega})$ pointwise in ω, which is the same as saying that the minimum rank over all ω is M. Finally, from the linear systems theory we know that there is a left polynomial inverse of a $L \times M$ polynomial matrix if and only if the gcd of all its $M \times M$ minors is a delay [20, 29]. $\bigtriangledown\bigtriangledown\bigtriangledown$

Due to a rather complicated relation between the starting filters $F(z)$ and $H(z)$ and the polyphase matrices $\mathbf{E}(z)$ and $\mathbf{R}(z)$, it is not clear how the conditions appearing in Theorem 1 can be translated into the corresponding conditions on the filters $F(z)$ and $H(z)$. Note that whenever the conditions for the existence of FIR FBPs are satisfied, these solutions are not unique. This is a consequence of the construction for left polynomial inverses of tall polynomial matrices, or equivalently right polynomial inverses of fat polynomial matrices [5]. In the next section we exploit this nonuniqueness in the process of constructing FIR zero-forcing fractionally spaced equalizers for communication channels.

3 Channel Equalization With Fractionally Spaced Equalizers

Consider the continuous time baseband communication system shown in Fig. 6. Information sequence $x(n)$, with symbol spacing T (rate $1/T$) is converted into an analog signal and after pulse shaping fed into the communication channel. This is shown in Fig. 6(a). Here $f_c(t)$ denotes the combined effect of the reconstruction filter from the D/A converter, pulse shaping filter as well as the continuous time channel. After passing through the channel, signal is corrupted by the additive noise and the received waveform $q_c(t)$ is sampled at the rate $(L/M)/T$ to produce the received sequence $q(n)$. If the ratio L/M is equal to 1, the equalizer at the receiver from Fig. 6(b) is called the symbol spaced equalizer (SSE). Several problems with this method have been pointed out in [17]. The receiver in this case becomes very sensitive to the phase shift at the sampling device;

also, sampling at exactly the symbol rate may create some aliasing problems. In addition to this, note that the zero-forcing SSE is nothing but the channel inverse, which is almost always IIR and sometimes introduces stability issues which can lead to severe channel noise amplification. For all these reasons, the preferred alternative is to keep $L > M$, giving rise to the receiver structure called the fractionally spaced equalizer (FSE) - see Fig. 6(b). The received sequence $q(n)$ with the denser spacing (higher rate) enters the fractionally spaced equalizer $h_{FSE}(n)$, which now has to operate at a slightly higher rate. Accompanied with this process, some rate reduction also needs to take place at the receiver so that the final sequence $\hat{x}(n)$ entering the decision device has exactly the same rate $1/T$ as the information sequence $x(n)$.

The purpose of the FSE at the receiver is to compensate for the distortion introduced by $f_c(t)$. If the FSE is designed so that in the absence of noise $\hat{x}(n) = x(n)$, then it is called the *zero-forcing equalizer* (**ZFE**). Note, however that the ZFE is not necessarily the best solution, since we need to take into account the effect of the additive noise as well. In addition to taking care of some problems of SSEs mentioned earlier, FSEs often provide FIR zero-forcing solutions, which are in general favorable to IIR solutions for the reasons of stability and complexity of implementation. Moreover, oversampling at the receiver often allows for *blind* channel identification and equalization [16, 13, 14].

In the case of vector signals and integer oversampling at the receiver (when L/M is an integer) it has been shown [26, 28] that FIR solutions (even those of minimum order) are not unique. This flexibility in the design of vector ZFEs was utilized to further reduce the noise at the receiver [26, 27, 28]. Here we deal with the case where the oversampling ratio L/M is not an integer but a rational number. This leads to FSEs with fractional oversampling, which are reviewed next.

It should be noted that even though there are some similarities between the underlying filter bank structures of the FSE system considered here and the discrete multitone (DMT) system [6, 8, 11], the two problems do not have much in common. DMT systems make use of the transmultiplexer-like structures, whereas our paper deals with the dual system (analysis/synthesis) and uses fractional decimators. In addition to that, FIR equalization in DMT systems is achieved by introducing some form of redundancy at the transmitter which eventually leads to the *bandwidth expansion*. In contrast, the systems with fractionally spaced equalizers in general do not introduce any bandwidth expansion, but require more computations at the receiver. In this paper we show that in most cases this computational overhead can be minimal since even the slight amount of oversampling often leads to FIR solutions. This should be compared to FSEs with integer over-

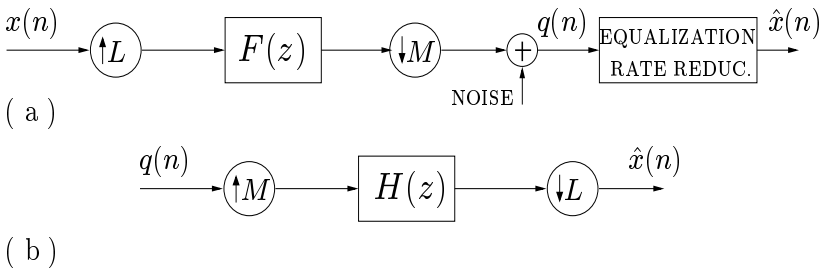

Figure 7: FSEs with fractional oversampling. (a) Discrete time model of the communication system. (b) Form of the proposed equalizer.

sampling where $L/M = 2$ is the minimum oversampling ratio and thus results in the minimum computational overhead. FSEs with fractional oversampling were also treated by Ding and Qiu in the context of blind identification [3]. Although the authors there use a different notation, it can be shown that the problem formulation in [3] is equivalent to the one presented here.

3.1 FSEs with fractional oversampling

As we did before, in the following we assume that $L > M$ and that L and M are coprime. Consider again Fig. 6(a) in the absence of noise. We can see that

$$q(n) = q_c(n\frac{M}{L}T) = \sum_{k=-\infty}^{\infty} x(k) f_c(n\frac{M}{L}T - kT). \tag{10}$$

By defining the discrete time sequence $f(n) \stackrel{\triangle}{=} f_c(nT/L)$, which is actually the function $f_c(t)$ sampled L times more densely than at integers, we have

$$q(n) = \sum_{k=-\infty}^{\infty} x(k) f(nM - kL). \tag{11}$$

This identity is incorporated in Fig. 7(a) where we show the discrete time model of the communication system from Fig. 6.

The discrete time noise appearing in Fig. 7(a) is obtained by sampling the corresponding continuous time noise from Fig. 6(a) at the rate L/MT. In the following we focus on the box in Fig. 7(a) labeled "equalization and rate reduction". Recalling that in the zero-forcing setting the goal of this block is to make $\hat{x}(n) = x(n)$ in the absence of noise, we conclude that this block needs to incorporate a right FBP of $F(z)$ with respect to L/M. In other words, we search for the equalizer of the form shown in Fig. 7(b). Of special interest are FIR solutions, and nonuniqueness of these solutions is exploited in the following.

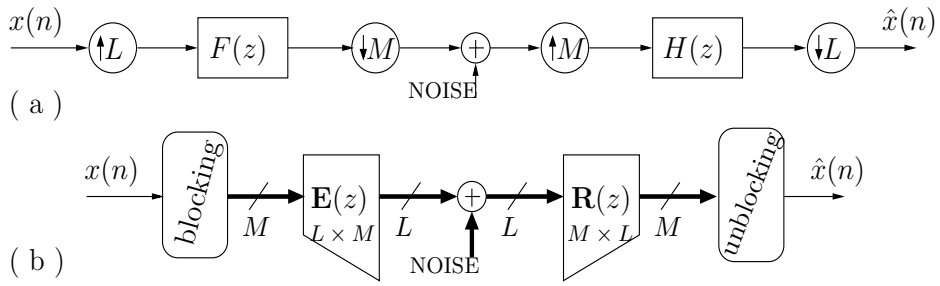

Figure 8: Communication system with FSEs. (a) FBP form. (b) Multichannel equivalent form.

3.2 Optimizing FIR RFBPs for channel equalization

It follows from the previous discussion that the discrete time equivalent communication system with fractionally oversampled FSEs can be drawn as in Fig. 8(a), which in turn can be equivalently presented as in Fig. 8(b). Matrices $\mathbf{E}(z)$ and $\mathbf{R}(z)$ are given by (8) and construction of the FSE $H(z)$ amounts to finding the appropriate left inverse $\mathbf{R}(z)$ of the matrix $\mathbf{E}(z)$. In the following we assume that the equivalent channel $f_c(t)$ is of finite length, which implies that $\mathbf{E}(z)$ is a polynomial matrix. In practice, this is achieved by applying one of the several methods for channel shortening [1] before equalization. We look for FIR equalizers, implying that the corresponding polyphase matrix $\mathbf{R}(z)$ should be polynomial as well. Since the solution to this problem is not unique, we try to find the one that performs favorably with respect to the noise amplification at the receiver. Treatment of a similar problem can be found in [24, 27].

Let $\mathbf{E}(z)$ have an FIR left inverse and consider its Smith form [5]

$$\mathbf{E}(z) = \mathbf{U}(z)\mathbf{\Gamma}(z)\mathbf{V}(z). \tag{12}$$

Here $\mathbf{U}(z)$ and $\mathbf{V}(z)$ are $L \times L$ and $M \times M$ unimodular matrices [5] and $\mathbf{\Gamma}(z)$ is a $L \times M$ diagonal matrix. The elements on its diagonal are nonzero constants or delays, but without loss of generality we can assume that they are all constants. In other words, $\mathbf{\Gamma}(z) = [\mathbf{\Gamma} \;\; \mathbf{0}]^T$, where $\mathbf{\Gamma}$ is a $M \times M$ constant diagonal matrix. Now from (12) we have that the general form of an FIR left inverse of $\mathbf{E}(z)$ is given by

$$\mathbf{R}(z) = \mathbf{V}^{-1}(z)[\underbrace{\mathbf{\Gamma}^{-1}}_{M} \;\; \underbrace{\mathbf{A}(z)}_{L-M}]\mathbf{U}^{-1}(z), \tag{13}$$

where $\mathbf{A}(z)$ is *any* $M \times (L-M)$ polynomial matrix. It is important to note that the unimodular matrices $\mathbf{U}(z)$ and $\mathbf{V}(z)$ in (12) are not unique so the form (13) can be made slightly more general by including the different choices for $\mathbf{U}(z)$ and $\mathbf{V}(z)$. However, complete parameterization of the Smith form remains an open problem. Therefore, in the following we assume that a particular

decomposition (12) has been chosen. Also note that any choice of $\mathbf{A}(z)$ in (13) produces a valid FIR ZFE $H(z)$, but there will be an $\mathbf{A}(z)$ (of a given order $N_A - 1$) that minimizes the noise component of $\hat{x}(n)$. In order to find such $\mathbf{A}(z)$ we consider the equivalent of Fig. 8(b) for the noise signal, shown in Fig. 9(a). Defining the polynomial matrices $\mathbf{D}_0(z)$ and $\mathbf{D}_1(z)$ to be

$$[\underbrace{\mathbf{D}_0^T(z)}_{M} \quad \underbrace{\mathbf{D}_1^T(z)}_{L-M}]^T = \mathbf{D}(z) \stackrel{\triangle}{=} \mathbf{U}^{-1}(z) \tag{14}$$

we can see that $\mathbf{R}(z)$ from (13) can be rewritten as

$$\mathbf{R}(z) = \mathbf{V}^{-1}(z)\mathbf{\Gamma}^{-1}\mathbf{D}_0(z) + \mathbf{V}^{-1}(z)\mathbf{A}(z)\mathbf{D}_1(z). \tag{15}$$

Defining $\mathbf{B}(z) \stackrel{\triangle}{=} \mathbf{V}^{-1}(z)\mathbf{A}(z)$ we can now redraw Fig. 9(a) as in Fig. 9(b). The problem of finding the optimal $\mathbf{A}(z)$ is therefore transformed into the one of finding the optimal $\mathbf{B}(z)$ of order $N_B - 1 = N_A - 1 + \text{ord}\{\mathbf{V}^{-1}(z)\}$, where the operator ord$\{\cdot\}$ denotes the order of a polynomial matrix. From Fig. 9(b) we see that the optimal $\mathbf{B}(z)$ is nothing but a matrix Wiener filter [15] of order $N_B - 1$ for recovering the desired vector signal $-\mathbf{u}(n)$ given the vector process $\mathbf{v}(n)$.

In order to solve for the optimal $\mathbf{B}(z)$ we are first going to write matrix convolutions as products of larger block matrices. Let $\mathbf{C}(z) \stackrel{\triangle}{=} \mathbf{V}^{-1}(z)\mathbf{\Gamma}^{-1}\mathbf{D}_0(z)$ and let the matrices $\mathbf{B}_i$, $\mathbf{C}_i$ and $\mathbf{D}_i$ represent the impulse responses of $\mathbf{B}(z)$, $\mathbf{C}(z)$ and $\mathbf{D}_1(z)$ respectively. Next define the $M \times N_C L$ matrix $\mathcal{C}$ and the $(L-M)N_B \times L(N_B + N_D - 1)$ matrix $\mathcal{D}_1$ as

$$\begin{aligned} \mathcal{C} &\stackrel{\triangle}{=} [\mathbf{C}_0 \;\; \mathbf{C}_1 \;\; \cdots \;\; \mathbf{C}_{N_C-1}] \\ \mathcal{D}_1 &\stackrel{\triangle}{=} \begin{bmatrix} \mathbf{D}_0 & \dots & \mathbf{D}_{N_D-1} & \mathbf{0} & \dots & \mathbf{0} \\ \mathbf{0} & \mathbf{D}_0 & \dots & \mathbf{D}_{N_D-1} & \dots & \mathbf{0} \\ \vdots & & \ddots & & \ddots & \\ \mathbf{0} & \dots & \mathbf{0} & \mathbf{D}_0 & \dots & \mathbf{D}_{N_D-1} \end{bmatrix}. \end{aligned} \tag{16}$$

We also define the $N_B(L-M) \times 1$ vector process $\mathcal{V}(n)$ and the $M \times N_B(L-M)$ matrix $\mathcal{B}$ as

$$\begin{aligned} \mathcal{V}(n) &\stackrel{\triangle}{=} [\mathbf{v}^T(n) \;\; \mathbf{v}^T(n-1) \;\; \cdots \;\; \mathbf{v}^T(n-N_B+1)]^T, \\ \mathcal{B} &\stackrel{\triangle}{=} [\mathbf{B}_0 \;\; \mathbf{B}_1 \;\; \cdots \;\; \mathbf{B}_{N_B-1}]. \end{aligned} \tag{17}$$

By the orthogonality principle we have that $E\{\hat{\mathbf{e}}(n) \cdot \mathcal{V}^\dagger(n)\} = E\{[\mathcal{B}\mathcal{V}(n) + \mathbf{u}(n)]\mathcal{V}^\dagger(n)\} = \mathbf{0}$ (here $E\{\cdot\}$ denotes the expected value); therefore, we find the optimal $\mathcal{B}$ as

$$\mathcal{B} = -E\{\mathbf{u}(n)\mathcal{V}^\dagger(n)\} \cdot \mathcal{R}_{\mathcal{V}\mathcal{V}}^{-1}, \tag{18}$$

where $\mathcal{R}_{\mathcal{V}\mathcal{V}}$ is the autocorrelation matrix of $\mathcal{V}(n)$. Given the definitions (16) and referring to Fig. 9(b) we see that $\mathbf{u}(n) = \mathcal{C}\mathcal{E}_{N_C}$ and $\mathcal{V}(n) = \mathcal{D}_1\mathcal{E}_{N_D+N_B-1}$, where $\mathcal{E}_N$ denotes the $NL \times 1$ vector of

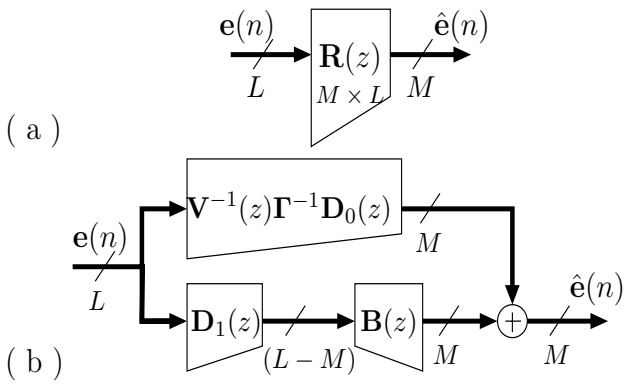

Figure 9: (a)-(b) Finding the optimal FIR RFBP. See text.

concatenated input noise vectors $\mathbf{e}(n-i)$, $0 \le i \le N-1$, namely

$$\mathcal{E}_N \stackrel{\triangle}{=} \left[\mathbf{e}^T(n) \;\; \mathbf{e}^T(n-1) \;\; \cdots \;\; \mathbf{e}^T(n-N+1)\right]^T.$$

Substituting these in (18) we have that the optimal $\mathbf{B}(z)$ is given by its impulse response matrix

$$\mathcal{B} = -\mathcal{C} \cdot \mathcal{R}_{\epsilon\epsilon}(1 : N_C L, :) \cdot \mathcal{D}_1^{\dagger} \cdot \left(\mathcal{D}_1 \cdot \mathcal{R}_{\epsilon\epsilon} \cdot \mathcal{D}_1^{\dagger}\right)^{-1}. \tag{19}$$

Here $\mathcal{R}_{\epsilon\epsilon}$ is a $L(N_B+N_D-1) \times L(N_B+N_D-1)$ autocorrelation matrix of the input noise process, and we employ Matlab's notation $\mathbf{W}(1:N,:)$ which represents the matrix consisting of the first N rows of $\mathbf{W}$.

3.3 MMSE equalizer

As we mentioned earlier, although the zero-forcing equalizer completely eliminates the channel distortion, the best equalizer $\mathbf{R}(z)$ of a given order $N_R - 1$ in Fig. 8(b) is the one that minimizes the mean-squared error between $x(n)$ and $\hat{x}(n)$. This is nothing but the Wiener filter for vector signals described in [15]. Consider Fig. 8(b). Let the matrices $\mathbf{E}_i$ and $\mathbf{R}_i$ denote the impulse responses of $\mathbf{E}(z)$ and $\mathbf{R}(z)$ respectively and let the $N_R L \times M(N_R+N_E-1)$ matrix $\mathcal{G}$ be defined as

$$\mathcal{G} \stackrel{\triangle}{=} \begin{bmatrix} \mathbf{E}_0 & \dots & \mathbf{E}_{N_E-1} & \mathbf{0} & \dots & \mathbf{0} \\ \mathbf{0} & \mathbf{E}_0 & \dots & \mathbf{E}_{N_E-1} & \dots & \mathbf{0} \\ \vdots & & \ddots & & \ddots & \\ \mathbf{0} & \dots & \mathbf{0} & \mathbf{E}_0 & \dots & \mathbf{E}_{N_E-1} \end{bmatrix}$$

It can be shown [15] that the MMSE solution for $\mathbf{R}(z)$ is given by its impulse response

$$\mathcal{P} \stackrel{\triangle}{=} [\mathbf{R}_0 \;\; \mathbf{R}_1 \;\; \cdots \;\; \mathbf{R}_{N_R-1}] = \mathcal{R}_{\mathcal{X}\mathcal{X}}(1:M,:) \cdot \mathcal{G}^{\dagger} \cdot \left(\mathcal{G} \cdot \mathcal{R}_{\mathcal{X}\mathcal{X}} \cdot \mathcal{G}^{\dagger} + \mathcal{R}_{ee}\right)^{-1}. \tag{20}$$

Here $\mathcal{R}_{\mathcal{X}\mathcal{X}}$ is a $M(N_R+N_E-1)\times M(N_R+N_E-1)$ autocorrelation matrix of the input sequence $x(n)$ and $\mathcal{R}_{ee}$ is a $N_RL\times N_RL$ autocorrelation matrix of the noise process.

Even though the MMSE method provides statistically the best solution, the equalizers based on zero-forcing are often preferred for simplicity reasons. Namely, comparing the two solutions (19) and (20) we see that as opposed to the MMSE method, the optimized FIR RFBP method does not require the knowledge of the signal autocorrelation matrix nor the noise variance, whenever the noise is uncorrelated. The latter can become a significant advantage, especially in the low signal to noise ratio (SNR) case, when the matrix inversion in (20) depends significantly on the noise power. This point is illustrated in the next subsection. Also, in some applications the transmitter might change the coding technique during the transmission (thus changing the signal covariance matrix), while the equalizer stages of the receiver might not have this information available. This would seriously affect the MMSE performance (20), however the optimal solution (19) would remain the same.

3.4 Performance evaluation

Using computer simulations, we compare the equalization performance of four different methods

1. Traditional IIR SSE (simply a channel inverse), which corresponds to the case of no oversampling at the receiver, i.e. when $L=M$ (we call this method **SSE**).
2. Simple FIR FSE method using plain RFBPs [without the optimization matrix $\mathbf{A}(z)$], as in Sec. 2.2 (**plain RFBP**).
3. Optimized FIR RFBP method described in Sec. 3.2 (**optimized RFBP**).
4. MMSE equalizer described in Sec. 3.3 (**MMSE**).

The channel sampled at integers was taken to be of the fourth order, with coefficients

$$1.0000 \quad 0.7599 \quad -0.2600 \quad -0.1200 \quad 0.5000$$

and the corresponding sequence $f(n)$ [$f_c(t)$ oversampled by L] was obtained by linear interpolation. Note that two of the four complex zeros of the minimum phase channel lie very close to the unit circle and thus the traditional SSE consists of a barely stable IIR filter which amplifies the channel noise. In the FSE implementations we considered the $L=5$ and $M=4$ case, so that the amount of computational overhead for the fractionally spaced equalizer (with respect to the symbol spaced one) was just 25%. The order of the MMSE solution $\mathbf{R}(z)$ given by (20) was $N_R-1=7$. For the

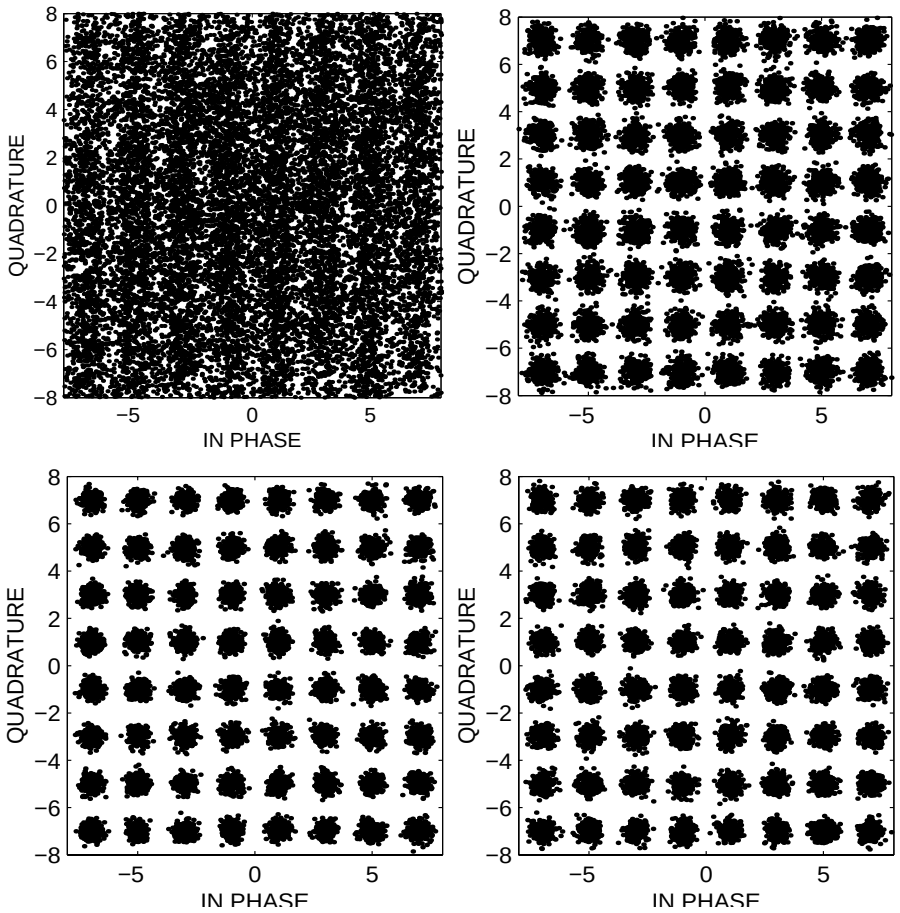

Figure 10: Equalization results. Clockwise, starting from upper left: SSE, plain FIR RFBP, optimized FIR RFBP and MMSE methods.

fairness of comparison, the optimized FIR RFBP given by (15) was chosen to be of the same order and thus the order of the linear estimator $\mathbf{B}(z)$ was $N_B - 1 = 3$.

The noise was taken to be white and the signal to noise ratio (SNR) measured at the input to the receiver was 29 dB. The obtained probabilities of error for the four methods were 0.0791, 1.4×10^{-3}, 1.19×10^{-5} and 5.0×10^{-6} respectively. The corresponding scattering diagrams for the input constellation of 64-QAM are shown clockwise in Fig. 10. The diagram presenting the probability of error in the four methods as a function of the SNR is shown in Fig. 11.

The simulation example shows that the improvement in performance achieved by exploiting the redundancy in the construction of FIR RFBPs can be significant. Also, both plain RFBP and optimized RFBP methods perform significantly better than SSE, at the expense of just 25% increase in the clock rate at the receiver. It can also be observed that the method of optimized RFBP equalization does not perform far from the optimal MMSE equalization of the same order,

while it requires no knowledge of the input statistics and the noise variance.

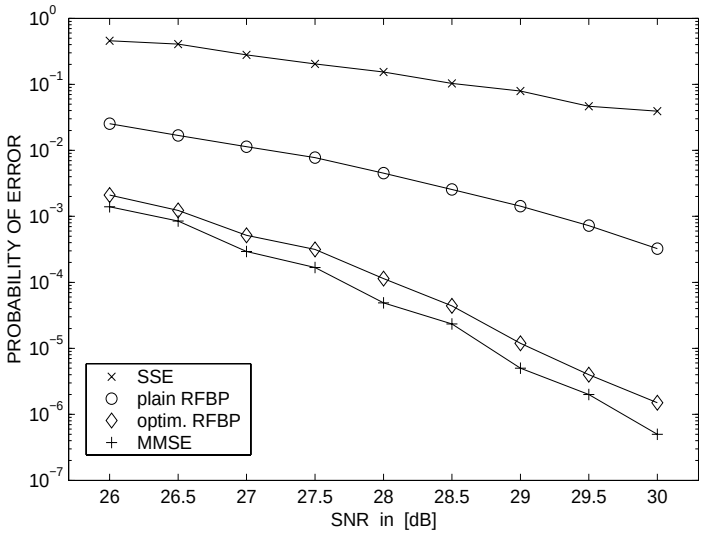

Figure 11: Probability of error as a function of SNR in the four equalization methods.

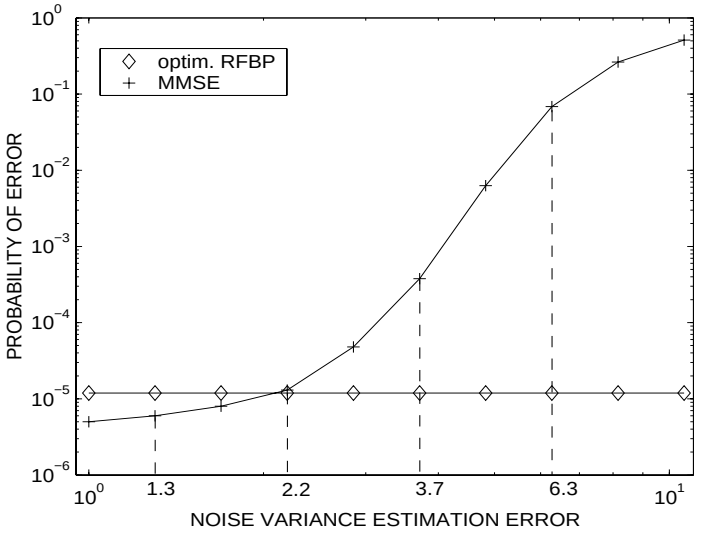

Figure 12: Probability of error as a function of noise variance discrepancy α.

In Fig. 12 we explore the sensitivity of the optimal MMSE equalizer to the estimate of the noise variance at the receiver. Let the ratio between the estimated and the actual noise variances be $\sigma_{est}/\sigma_{act} = \alpha$. In Fig. 12 we show the probability of error achieved using the equalization methods three and four as a function of the parameter α with a fixed SNR of 29 dB. We can see that whenever the noise variance gets overestimated by a factor of two or more, the MMSE equalizer

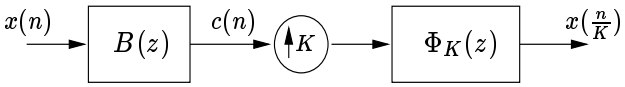

Figure 13: Interpolation of discrete signals using digital filtering. In the case of spline interpolation, $\phi_K(t)$ is an oversampled B-spline.

performance becomes comparable or even worse than the performance of the optimized FIR RFBP equalizer.

4 Interpolation of Oversampled Signals

4.1 Spline models in conventional interpolation

Given a discrete time signal $x(n)$ and a function $\phi(t)$, we can almost always assume that $x(n)$ is obtained by sampling at integers the continuous time signal $x(t)$ given by the model (2), i.e.

$$x(n) = \sum_{k=-\infty}^{\infty} c(k)\phi(n-k). \tag{21}$$

The only condition is that $\Phi(e^{j\omega})$, the discrete time Fourier transform of $\phi(n)$ is nonzero for all ω [21]. The driving coefficients $c(n)$ can be obtained via the inverse filter $1/\Phi(e^{j\omega})$, if it is stable. These driving coefficients can then be employed for signal reconstruction as in (2) or for the *interpolation* of discrete signals. The signal $x(n)$ interpolated by an integral factor K is obtained by sampling $x(t)$ from (2) K times more densely than at integers. Thus, the interpolation process for the signals admitting the model (21) is shown in Fig. 13, with $\phi_K(t) \stackrel{\triangle}{=} \phi(t/K)$ and $B(e^{j\omega}) \stackrel{\triangle}{=} 1/\Phi(e^{j\omega})$.

While in principle $\phi(t)$ can be chosen to be just about any function, various researchers have traditionally used continuously differentiable interpolating functions such as *B-splines* [4, 12] to insure some smoothness properties of the resulting interpolant. The mth order B-spline is given by the m-fold convolution of the unit pulse function

$$p(t) = \begin{cases} 1 & \text{for } t \in [0,1), \\ 0 & \text{otherwise} \end{cases}$$

with itself. The important property of B-splines is that they span the space of continuously differentiable functions - splines [12]. In other words, the $(m-1)$th derivative of $x(t)$ exists and is continuous if $x(t)$ admits the model (2), with $\phi(t)$ representing the mth order B-spline. The case when $m = 3$ is called cubic spline interpolation and it has received much attention in the image processing community [18]. The cubic spline $\phi(t)$ and its 3 times stretched version $\phi_3(t)$ are shown in Fig. 1.

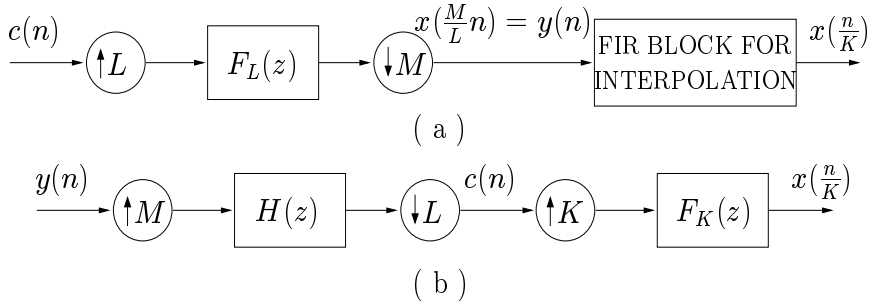

Figure 14: (a) Signal model and proposed interpolation. (b) Scheme for all-FIR interpolation.

Spline interpolation, though elegant, unfortunately comes at a certain price. It can be shown [18] that in this case the inverse filtering by $B(z) = 1/\Phi(z)$ in Fig. 13 is not only IIR but noncausal, so recursive implementation [18] is required. The authors in [22] consider one way of modifying the interpolation structure from Fig. 13 in order to avoid IIR filtering. Although the technique proposed there is shown to produce results very similar to the exact spline interpolation, it is still only an approximation of the exact method and results in the reduced degree of smoothness or irreversibility of the interpolant [22]. In [21], the same problem was considered from a slightly different point of view. It is shown that if $x(n)$ is a spline function *oversampled* by an integer amount, i.e. if $x(n)$ admits the model (21), with $\phi(n)$ being a B-spline oversampled by some integer, then the reconstruction prefilter $B(z)$ in Fig. 13 can be FIR and the system still produces the exact spline interpolant. In the following we extend this work by showing that even if $x(n)$ is a spline oversampled by an arbitrarily small (rational) amount, the all-FIR interpolation is still possible.

4.2 FBPs in all-FIR interpolation of oversampled signals

Let $x(t)$ be a third order spline given by the model (2). Consider the discrete time signal $y(n) = x(\frac{M}{L}n)$ (for $L > M$) which is obtained by oversampling $x(t)$ by a factor of L/M. The signal $y(n)$ can be constructed as shown in the first half of Fig. 14(a). Here $F_L(z)$ represents the z-transform of the sequence $\phi_L(n)$, which is obtained by sampling $\phi(t)$ L times more densely than at integers. Our task is to find an interpolation system as in Fig. 14(a) consisting of FIR filters only, that produces the interpolated version $x(\frac{n}{K})$, for an arbitrary integer K. The interpolation by a rational amount K_1/K_2 can in principle be thought of as an interpolation by K_1 followed by a simple decimation by K_2. Also, note that the oversampled signal $y(n)$ actually gets interpolated by a total factor of MK/L.

Figure 15: FIR interpolation example: a region of the image oversampled by $L/M = 6/5$ and its cubic spline interpolation by a factor of $MK/L = 5/3$ obtained using FIR filters.

Following the discussion from Sec. 2 we conclude that the driving sequence $c(n)$ can be recovered as shown in the first half of Fig. 14(b), where $H(z)$ is a RFBP of $F_L(z)$ with respect to L/M. It is often possible to find FIR solutions for $H(z)$ as explained in Sec. 2.2. After this is achieved, the interpolation by K is achieved as in the second half of Fig. 14(b), where $F_K(z)$ is obtained similarly by oversampling a cubic spline by a factor of K. Summarizing, we have achieved an all-FIR spline interpolation, with the only requirement being that the input signal admits a slightly oversampled model. By making $L = M + 1$ and choosing M large enough, this required overhead in the input sampling can be made insignificant.

In Fig. 15 we present an example of all-FIR cubic spline interpolation. In this example we used $L = 6$ and $M = 5$. The smaller image is a portion of the *Parrots* image, oversampled by 6/5. In other words, this signal satisfies the model in Fig. 14(a). It was obtained using the traditional cubic spline interpolation by a factor of 6/5. Employing the system described in Fig. 14(b) with an FIR filter $H(z)$ and $K = 2$, this image is next interpolated by a total factor of $MK/L = 5/3$ and the result is also shown in Fig. 13. We note that this is precisely the same result as the one obtained using recursive IIR filtering in traditional spline interpolation [18]. However, in this case we had to assume a certain signal model, which is not valid for an arbitrary signal. A possible remedy is to *approximate* the starting signal with the signal admitting the model and then proceed with the all-FIR interpolation. In the next section we define the approximation problem and derive

the solution.

5 Least Squares Signal Approximation

Consider the class $\mathcal{F}$ of discrete time signals $y(n)$ which can be modeled as the output of the system shown in Fig. 16(a). The signal model from Fig. 16(a) appears in several different contexts; for example see the left half of Fig. 7(a) or the left half of Fig. 14(a). Here, $c(n)$ is an arbitrary ℓ_2 sequence, and L and M are coprime integers satisfying $L > M$. The problem of least squares approximation is as follows. Given an arbitrary signal $x(n) \in \ell_2$, find a signal $y(n) \in \mathcal{F}$ such that the ℓ_2 distance between those two signals, namely

$$\sum_n |y(n) - x(n)|^2$$

is minimized. Obviously, this problem is the same as finding the optimal driving sequence $c(n)$. The reason for the restrictions on L and M is similar as before; if L and M have a common factor, say P, then the model reduces to the similar one with the expander and decimator ratios L/P and M/P respectively, and $F(z)$ replaced by its zeroth polyphase component of order P. On the other hand if $L < M$, the class $\mathcal{F}$ almost always incorporates all ℓ_2 signals and the approximation problem becomes degenerate. Note that $y(n)$ is nothing but the *orthogonal projection* of $x(n)$ onto $\mathcal{F}$.

In order to solve the least squares problem, notice that the structure from Fig. 16(a) can be equivalently redrawn as in Fig. 16(b). Here $F_i(z)$ for $0 \leq i \leq M-1$ are the Type-1 polyphase components of order M of $F(z)$. Next, notice that the structure between $c(n)$ and the input to filter $F_i(z)$ is nothing but a cascade of an expander by L, delay z^{-i} and a decimator by M. Using the identity shown in Fig. 4(a), we can redraw Fig. 16(b) as in Fig. 16(c). We also used the fact that L and M are coprime, and integers l and m are chosen such that (6) is satisfied. Filters $U_i(z)$ are defined as

$$U_i(z) \stackrel{\triangle}{=} z^{-im} \cdot F_i(z).$$

Now, notice that the subsequences $c_i(n)$ represent a complete partitioning of $c(n)$, i.e. $c(n)$ can be recovered from $c_i(n)$ as shown in the right part of Fig. 18(a). This is a consequence of the fact that l and M are coprime as well. Therefore, the problem of finding the optimal driving sequence $c(n)$ in Fig. 16(a) is equivalent to the problem of finding the optimal driving sequences $\{c_i(n)\}$ for $0 \leq i \leq M-1$ in Fig. 16(c). This problem represents a special, uniform case of a more general

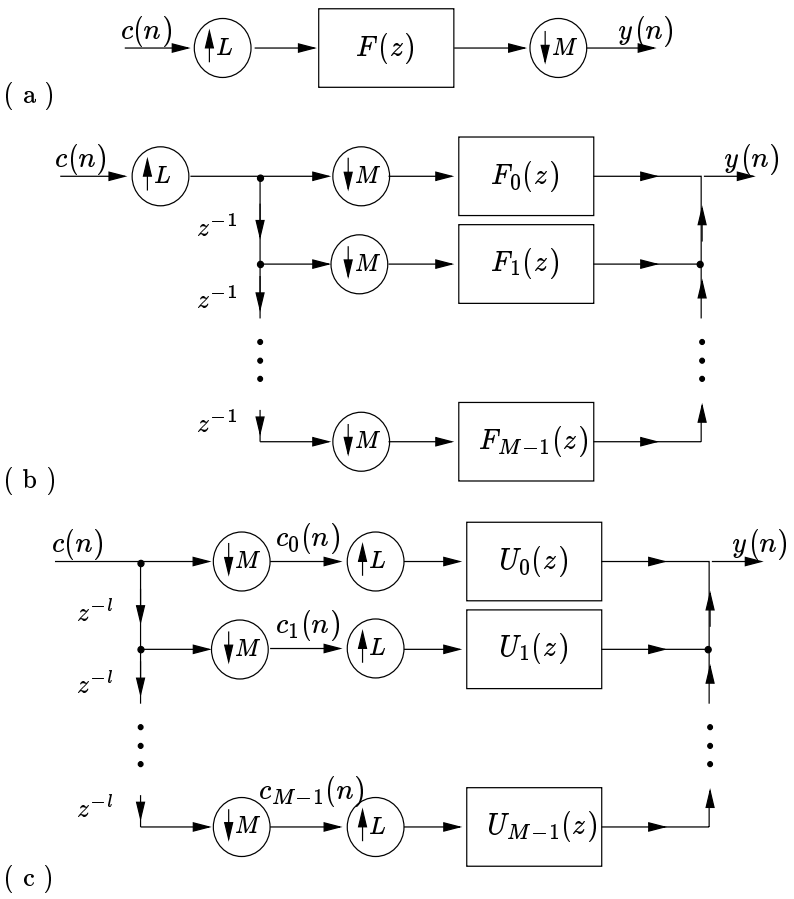

Figure 16: Least squares problem. (a) Signal model. (b)-(c) Equivalent drawing.

multichannel, nonuniform problem considered in [25]. Also, it can be viewed as a special case of the least squares problem considered in the MIMO biorthogonal partner setting [26].

Consider Fig. 17(a), with the vector sequence $\mathbf{c}(n)$ and MISO filter $\mathbf{U}(z)$ defined by

$$\begin{aligned}\mathbf{c}(n) &\stackrel{\triangle}{=} [c_0(n) \;\; c_1(n) \;\; \cdots \;\; c_{M-1}(n)]^T \\ \mathbf{U}(z) &\stackrel{\triangle}{=} [U_0(z) \;\; U_1(z) \;\; \cdots \;\; U_{M-1}(z)].\end{aligned}$$

It is easily seen that the signal model in Fig. 17(a) corresponds to the one in Fig. 16(c) and thus the one in Fig. 16(a). According to the results in [26], the solution to the corresponding least squares approximation problem is unique and is given by the structure shown in Fig. 17(b). The SIMO filter $\mathbf{V}(z)$ is defined by

$$\mathbf{V}(z) \stackrel{\triangle}{=} [V_0(z) \;\; V_1(z) \;\; \cdots \;\; V_{M-1}(z)]^T,$$

and can be found as

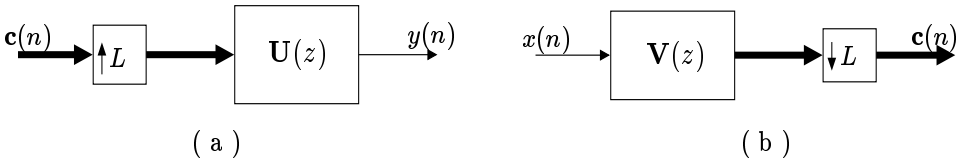

Figure 17: Least squares problem revisited in MIMO biorthogonal partner setting. (a) Signal model. (b) Least squares approximation.

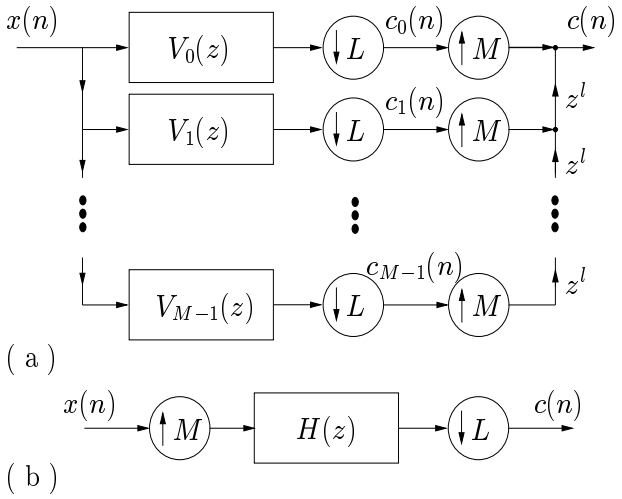

Figure 18: (a)-(b) Solution to the least squares problem.

$$\mathbf{V}(z) = \left([\tilde{\mathbf{U}}(z) \cdot \mathbf{U}(z)]_{\downarrow L \uparrow L} \right)^{-1} \tilde{\mathbf{U}}(z). \tag{22}$$

The notation $\tilde{\mathbf{U}}(z)$ stands for $\mathbf{U}^{*T}(1/z^*)$; in other words, on the unit circle this is nothing but a transpose-conjugate. Note that two of the necessary conditions for the existence of the matrix inverse in (22) are $L \geq M$ and $\left[|F_i(e^{j\omega})|^2\right]_{\downarrow L} > 0$ for all ω and for $0 \leq i \leq M-1$. However, they are not sufficient. On the other hand, if the matrix in question is not of full rank, we can use the Moore-Penrose generalized inverse (pointwise in ω) instead.

Representing the SIMO system $\mathbf{V}(z)$ in the form of a filter bank, we can redraw the solution from Fig. 17(b) as in Fig. 18(a), which also combines the optimal subsequences $\{c_i(n)\}$ back into the driving sequence $c(n)$. We can further simplify this system as shown in Fig. 18(b), using a similar method as in Fig. 16. Here, $H(z)$ is the optimum projection prefilter and is defined by

$$H(z) \triangleq \sum_{i=0}^{M-1} z^{i(Mm+1)} \cdot V_i(z^M).$$

Summarizing, the solution to the least squares approximation problem defined by the signal model in Fig. 16(a) is given by the structure in Fig. 18(b). Note that $H(z)$ is a particular RFBP of

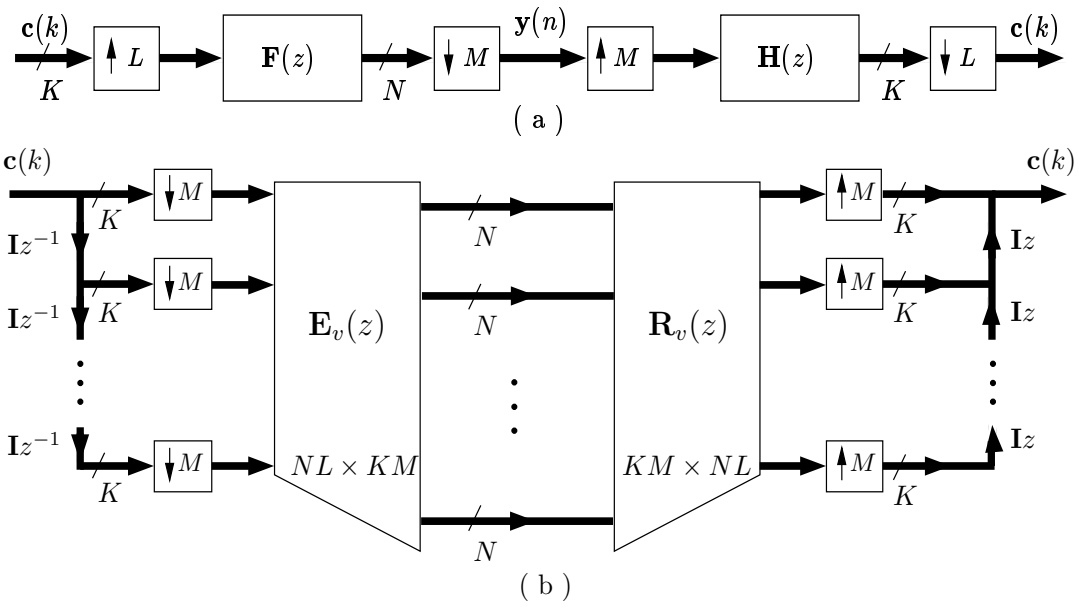

Figure 19: (a) Definition of vector FBPs. (b) Construction of vector FBPs.

$F(z)$ with respect to L/M, since the cascade of the systems from Fig. 16(a) and Fig. 18(b) is the identity.

6 Vector Signals

The problem of signal reconstruction discussed in Sec. 2 was originally posed for scalar signals. However, an analogous problem can be considered in the case of vector signals as well. Suppose that a $N \times 1$ vector signal $\mathbf{x}(t)$ admits the model

$$\mathbf{x}(t) = \sum_{k=-\infty}^{\infty} \mathbf{\Phi}(t-k)\mathbf{c}(k), \tag{23}$$

where $\mathbf{c}(k)$ is a $K \times 1$ vector driving sequence and $\mathbf{\Phi}(t)$ is a $N \times K$ matrix model function. We consider the discrete vector signal $\mathbf{y}(n)$ obtained by sampling $\mathbf{x}(t)$ at multiples of M/L. Thus we have $\mathbf{y}(n) = \mathbf{x}(nM/L)$ and the structure producing $\mathbf{y}(n)$ is shown on the left-hand side of Fig. 19(a). Here, $\mathbf{F}(z)$ is a z-transform of the integer samples of a $N \times K$ matrix function $\mathbf{F}(t) \stackrel{\triangle}{=} \mathbf{\Phi}(t/L)$. The problem of vector signal reconstruction can now be solved using the structure on the right-hand side of Fig. 19(a). The matrix transfer function $\mathbf{H}(z)$ for which the complete system shown in Fig. 19(a) is identity is called a right *vector* fractional biorthogonal partner (**RVFBP**) with respect to the ratio L/M. In this case we call $\mathbf{F}(z)$ a left *vector* fractional biorthogonal partner (**LVFBP**) with respect to L/M.

Similarly as before, we are usually concerned with the case when L and M are coprime, since otherwise we can reduce both the expander and decimator by a common factor. Using the equivalent reasoning as in the scalar case (Sec. 2), we conclude that the system from Fig. 19(a) can be equivalently redrawn as in Fig. 19(b), where the block polyphase matrices (for vector signals) $\mathbf{E}_v(z)$ and $\mathbf{R}_v(z)$ have a form similar to (8). The only difference is that the scalar polyphase components of filters $\{P_k(z)\}$ and $\{Q_k(z)\}$ are replaced by the $N \times K$ and $K \times N$ matrix polyphase components of the corresponding matrix filters $\{\mathbf{P}_k(z)\}$ and $\{\mathbf{Q}_k(z)\}$, defined similarly as in the scalar case (7). This discussion leads to the conditions for the existence of FIR or just stable RVFBPs, which are summarized in the following theorem.

Theorem 2. Given a $N \times K$ matrix transfer function $\mathbf{F}(z)$ and two coprime integers L and M, there exists a *stable* right vector fractional biorthogonal partner of $\mathbf{F}(z)$ if and only if $NL > KM$, and the minimum rank of $\mathbf{E}_v(e^{j\omega})$ [from Fig. 19(b)] pointwise in ω is M. For an FIR matrix filter $\mathbf{F}(z)$ there exists an *FIR* right vector fractional biorthogonal partner if and only if $NL > KM$, and the greatest common divisor (gcd) of all the $KM \times KM$ minors of $\mathbf{E}_v(z)$ is a delay. Analogous results hold for left vector FBPs as well.

The proof of this theorem is completely equivalent to the proof of Theorem 1, and is therefore omitted. Notice that the necessary condition $L > M$ from the scalar case here gets modified into a more general condition $NL > KM$. Similar to the scalar case, we conclude that whenever FIR VFBPs exist they are not unique. However, the degrees of freedom that can be used in the construction of FIR VFBPs now depend on the difference $NL - KM$ rather than $L - M$.

In accordance with the discussion in Sec. 3.1, we can define the problem of *vector* channel equalization using fractionally oversampled MIMO FSEs (see also [26] for MIMO FSEs with integral oversampling). The MIMO channels occur naturally in the applications with multiple transmit and/or receive antennas. The optimization of FIR MIMO FSEs in this setting can be made along the same lines as in Sec. 3.2, keeping in mind that the degrees of freedom come from the fact that $NL > KM$.

The other two applications of FBPs, considered in Sec. 4 and Sec. 5 can also be extended easily to the case of vector signals. The interpolation of vector signals has the application whenever the task is to asses the values of some vector-valued process at the instances between consecutive measurements. Of course, in order for the theory of linear interpolation (described in Sec. 4 in the case of scalar signals) to be applicable, the unknown continuous time vector process should be assumed to satisfy a model of the form similar to (23). As for the least squares signal approximation,

problem formulation is the same regardless of the dimensionality of the signals, so the extension is straightforward and a similar problem was treated in the MIMO (not fractional) biorthogonal partner setting in [26].

7 Concluding Remarks

The recent theory of biorthogonal partners in the scalar and vector case was derived from the signal models with integral amount of oversampling. In this paper we provide an extension of these results to the case when the oversampling amount is fractional. One of the main conclusions drawn here is that fractional biorthogonal partners always allow for additional flexibility in the design of FIR solutions, as long as those solutions exist. This fact was further explored in the setting of fractionally oversampled FSEs where we derived the optimal FIR solutions from the perspective of noise reduction. Several other applications of fractional biorthogonal partners were considered as well, including all-FIR signal interpolation and least squares signal approximation. The theory of FBPs was also extended to the case of vector signals.

References

[1] N. Al-Dhahir and J. M. Cioffi, "Efficiently computed reduced-parameter input-aided MMSE equalizers for ML detection: A unified approach," *IEEE Trans. Info. Theory*, vol. 42(5), pp. 903-915, May 1996.

[2] A. Aldroubi and M. Unser, "Oblique projections in discrete signal subspaces of ℓ_2 and the wavelet transform," Proc. SPIE, vol. 2303, *Wavelet applications in signal and image processing, II*, pp. 36-45, San Diego, CA, 1994.

[3] Z. Ding and L. Qiu, "Blind MIMO channel identifiability from second order statistics," in *Proc. Conf. on Decision and Control*, Sydney, Australia, Dec. 2000.

[4] H. S. Hou and H. C. Andrews, "Cubic splines for image interpolation and digital filtering," *IEEE Trans. Acoust., Speech, Signal Processing*, vol. ASSP-26, pp. 508-517, 1978.

[5] T. Kailath, *Linear Systems*. Prentice Hall, Inc., Englewood Cliffs, N.J., 1980.

[6] I. Kalet, "Multitone modulation," in *Subband and Wavelet Transforms: Design and Applications*, A. N. Akansu and M. J. T. Smith, Eds. Boston, MA: Kluwer, 1995.

[7] J. Kovačević and M. Vetterli, "Perfect reconstruction filter banks with rational sampling factors," *IEEE Trans. Signal Processing*, vol. 41(6), pp. 2047-2066, June 1993.

[8] Y.-P. Lin and S.-M. Phoong, "ISI-free FIR filterbank transceivers for frequency-selective channels," *IEEE Trans. Signal Processing*, vol. 49(11), pp. 2648-2658, Nov. 2001.

[9] K. Nayebi, T. P. Barnwell, III and M. J. T. Smith, "The design of perfect reconstruction nonuniform band filter banks," *Proc. ICASSP*, Toronto, Canada, May 1991.

[10] J. G. Proakis, *Digital Communications*. McGraw-Hill, New York, 1995.

[11] C. B. Ribeiro, M. L. R. de Campos and P. S. R. Diniz, "FIR equalizers with minimum redundancy," *Proc. ICASSP*, Orlando, FL, May 2002.

[12] I. J. Schoenberg, *Cardinal Spline Interpolation*. SIAM, 1973.

[13] D. T. M. Slock, "Blind fractionally-spaced equalization, perfect-reconstruction filter banks and multichannel linear prediction," in *Proc. ICASSP*, Adelaide, Australia, April 1994.

[14] D. T. M. Slock, "Blind joint equalization of multiple synchronous mobile users using oversampling and/or multiple antennas," in *Proc. 28th Asilomar Conference on Signals, Systems and Computers*, Pacific Grove, CA, Oct. 1994.

[15] C. W. Therrien, *Discrete Random Signals and Statistical Signal Processing*. Prentice-Hall, Englewood Cliffs, NJ, 1992.

[16] L. Tong, G. Xu and T. Kailath, "A new approach to blind identification and equalization of multipath channels," in *Proc. 25th Asilomar Conference on Signals, Systems and Computers*, Pacific Grove, CA, Nov. 1991.

[17] J. R. Treichler, I. Fijalkow and C. R. Johnson, Jr., "Fractionally spaced equalizers: how long should they really be?," *IEEE Signal Processing Magazine*, pp. 65-81, May 1996.

[18] M. Unser, A. Aldroubi, and M. Eden, "B-spline signal processing: Part I - Theory," *IEEE Trans. Signal Processing*, vol. 41, pp. 821-833, Feb. 1993.

[19] P. P. Vaidyanathan, *Multirate Systems and Filter Banks*. Prentice-Hall, Englewood Cliffs, NJ, 1995.

[20] P. P. Vaidyanathan and T. Chen, "Role of anticausal inverses in multirate filterbanks - Part I: System-theoretic fundamentals," *IEEE Trans. Signal Proc.*, vol. 43(5), May 1995.

[21] P. P. Vaidyanathan and B. Vrcelj, "Biorthogonal partners and applications," *IEEE Trans. Signal Processing*, vol. 49(5), pp. 1013-1027, May 2001.

[22] B. Vrcelj and P. P. Vaidyanathan, "Efficient implementation of all-digital interpolation," *IEEE Trans. Image Processing*, vol. 10(11), pp. 1639-1647, Nov. 2001.

[23] B. Vrcelj and P. P. Vaidyanathan, "Fractional biorthogonal partners and application to signal interpolation," *Proc. ISCAS*, Scottsdale, AZ, May 2002.

[24] B. Vrcelj and P. P. Vaidyanathan, "Fractional biorthogonal partners in fractionally spaced equalizers," *Proc. ICASSP*, Orlando, FL, May 2002.

[25] B. Vrcelj and P. P. Vaidyanathan, "Least squares signal approximation using multirate systems: multichannel nonuniform case," in *Proc. 35th Asilomar Conference on Signals, Systems and Computers*, Pacific Grove, CA, Nov. 2001.

[26] B. Vrcelj and P. P. Vaidyanathan, "MIMO biorthogonal partners and applications," *IEEE Trans. Signal Processing*, vol. 50(3), pp. 528-543, Mar. 2002.

[27] B. Vrcelj and P. P. Vaidyanathan, "On the general form of FIR MIMO biorthogonal partners," in *Proc. 35th Asilomar Conference on Signals, Systems and Computers*, Pacific Grove, CA, Nov. 2001.

[28] B. Vrcelj and P. P. Vaidyanathan, "Theory of MIMO biorthogonal partners and their application in channel equalization," in *Proceedings ICC*, Helsinki, Finland, June 2001.

[29] X.-G. Xia, "New precoding for intersymbol interference cancellation using nonmaximally decimated multirate filterbanks with ideal FIR equalizers," *IEEE Trans. Signal Processing*, vol. 45(10), pp. 2431-2441, Oct. 1997.